A component map tuning method for performance prediction and diagnostics of gas turbine compressors

TSOUTSANIS, Elias <http://orcid.org/0000-0001-8476-4726>, MESKIN, Nader, BENAMMAR, Mohieddine and KHORASANI, Khashayar

Published version

TSOUTSANIS, Elias, MESKIN, Nader, BENAMMAR, Mohieddine and KHORASANI, Khashayar (2014). A component map tuning method for performance prediction and diagnostics of gas turbine compressors. Applied Energy, 135, 572-585.

A component map tuning method for performance prediction and diagnostics of gas turbine compressors

Elias Tsoutsanis[a], Nader Meskin[a,*], Mohieddine Benammar[a], Khashayar Khorasani[b]

[a] *Department of Electrical Engineering, College of Engineering, Qatar University, Doha, Qatar*
[b] *Department of Electrical and Computer Engineering, Concordia University, Montreal, Canada*

Abstract

In this paper, a novel compressor map tuning method is developed with the primary objective of improving the accuracy and fidelity of gas turbine engine models for performance prediction and diagnostics. A new compressor map fitting and modelling method is introduced to simultaneously determine the best elliptical curves to a set of compressor map data. The coefficients that determine the shape of the compressor map curves are analyzed and tuned through a multi-objective optimization scheme in order to simultaneously match multiple sets of engine performance measurements. The component map tuning method, that is developed in the object oriented Matlab Simulink environment, is implemented in a dynamic gas turbine engine model and tested in off-design steady state and transient as well as degraded operating conditions. The results provided demonstrate and illustrate the capabilities of our proposed method in refining existing engine performance models to different modes of the gas turbine operation. In addition, the excellent agreement between the injected and the predicted degradation of the engine model demonstrates the potential of the proposed methodology for gas turbine diagnostics. The proposed method can be integrated with the performance-based tools for improved condition monitoring and diagnostics of gas turbine power plants.

Keywords: Component map, Model adaptation, Performance prediction, Gas turbine, Condition monitoring

Highlights

- A method for fitting rotated elliptical curves to compressor performance map data is presented.
- The proposed fitting method is integrated into a dynamic model of a gas turbine.
- The performance of the method is tested in steady state and transient conditions of gas turbine.
- The proposed method is used to diagnose compressor fouling from transient data.

*Corresponding author
Email address: nader.meskin@qu.edu.qa (Nader Meskin)

- The maintenance cost attributed by the accuracy of the proposed method is assessed as compared to other methods.

Nomenclature

Symbols

a	semi-major axis of an ellipse
A	matrix of elements α
b	semi-minor axis of an ellipse
f	flow rate
g	generic form of map's sub/coefficients
m	corrected mass flow rate
$\dot{m}$	mass flow rate
$\dot{m}'$	mass flow rate from plenum
n	total number of operating points per speed line
N	corrected shaft rotational speed
p	pressure
p'	pressure from plenum
P	power
q	total number of speed lines
sm	surge margin
T	temperature
T'	temperature from plenum
$\mathbf{u}$	ambient and operating conditions vector
x	coordinate of an ellipse in x-axis
$\mathbf{X}$	component characteristics vector
y	coordinate of an ellipse in y-axis
$\mathbf{Y}$	measurement vector

Greek

α	element of matrix A
Γ	mass flow capacity
ϵ	average prediction error
η	isentropic efficiency
θ	angle of rotated ellipse

π	pressure ratio
σ	spread, smooth parameter

Subscript

act	actual
amb	ambient
c	compressor
cl	clean
d	diffuser
deg	degraded
des	design point
f	fuel
i	order of the polynomial, number of the speed lines
inj	injected
j	number of the operating points
max	maximum
pred	predicted
pt	power turbine
r	reference engine
s	steady state
surge	surge point
t	turbine
tr	transient
w	weighted
0	fixed coordinate, θ=0
2	compressor inlet
3	compressor exit
4	combustor exit
5	turbine exit
6	power turbine exit
7	exhaust

1. Introduction

Gas turbine performance simulation, diagnosis and prognosis are strongly dependent on detailed understanding of the engine component behavior. Typically the bevahior of an engine component is represented

by performance maps which are the Original Equipment Manufacturer's (OEM) proprietary design information. At the off-design conditions, the quality of engine component maps is vital for the accuracy of gas turbine performance and diagnostic models. Special interest is given to compressors since they can generate various operational problems such as surge, stall and flutter, although their operating line is determined by the turbine characteristics. Maps can also be determined by flow analysis schemes such as the Stream Line Curvature (SLC) method [1] or high fidelity Computational Fluid Dynamics approaches (CFD) if the geometry of the compressor is known.

Gas turbine users do not have access to the context of such maps and their involvement is only limited to the use of tailored to customer decks for performance computations. The above limitations have recently motivated gas turbine research community to explore alternative methods [2],[3],[4] for representing the compressor maps in order to improve the accuracy of the performance prediction.

Some researchers have focused on the map representation itself, while others have implemented compressor map methods further in performance models of gas turbines. Kurzke [5] introduced auxiliary coordinates (beta lines), having no physical significance, which are superimposed in order to address the non-uniqueness and ill-conditioning issues of the compressor map shapes. Jones *et al.* [6] and Sethi *et al.* [7] introduced quasi-physics-based backbone compressor mapping approaches. The work by Drummond and Davison [8] examined the shape variance of the compressor maps for a wide range of compressor shapes and related them to the physical processes. A promising data-based method for the component performance which uses Back Propagation Neural Networks (BPNN) has been developed by Yu *et al.* [2]. The general regression neural networks (GRNN) and Multi Layer Perception (MLP) approaches that have been suggested by M. Gholamrezaei and K. Ghorbanian [9] provide good prediction of the compressor map shape. The accuracy and performance of the above methods depend on the quality and quantity of the available engine data from the engine manufacturers or the engine users.

One of the most commonly used methods involves scaling and shifting the shape of a similar compressor map through optimization techniques such that it matches the targeted engine measurements. Such a scaling method was proposed by Kong *et al.* [10] on the assumption that the implemented map has a very similar shape to the actual map. A combined hybrid approach that was developed by Kong *et al.* [3] takes advantage of Genetic Algorithms (GA) for determining the coefficients of the polynomials used in the system identification method. Recently Li *et al.* [4] have suggested a unique set of scaling coefficients for each line of the constant speed and efficiency to capture nonlinear effects. This method yields a higher accuracy than the traditional scaling methods at operating points away from the design point of the engine.

Although the advantages and benefits of the above approaches in engine performance prediction are extensive, the trade-offs between key parameters such as the operating range, accuracy, complexity and computational time are still debated and worth further investigation. Data-based approaches such as Neural Networks (NN) [2, 9] and GA [10, 11] might provide improved prediction accuracy with the compressor map

data and/or engine measurements; however they suffer from the extensive training and non-uniqueness of the solution, respectively. On the other hand, in diagnostics systems and approaches both GA and NN can be designed to be robust due to performing prior signal processing operations [12]. Since transient data are normally acquired online at reasonably high rates the former methods cannot be used effectively when integrated into a dynamical engine model. This is specially the case for real-time performance prediction of a gas turbine. Therefore, it is essential to develop a robust, formally validated, generic and computationally efficient approach for representing a compressor map that when empowered with model adaptation will be able to predict a gas turbine's performance at off-design steady state and transient conditions.

In this paper, a compressor map generation method for improving the accuracy of the gas turbine performance prediction and diagnostics is developed. In contrast to the earlier work [13], where the shape of a compressor map was expressed by mathematical equations of an ellipse with fixed center and no rotation, this study proposes a more sophisticated and accurate approach by considering rotation of the ellipses and transformation of its coordinates. This method is integrated into a dynamic engine model that is developed in the Matlab/Simulink environment. The dynamic engine model itself and its validation against the gas turbine simulation software PROOSIS [14] were the subject of our earlier work [15]. Moreover, the application is not only tested to the steady state off-design operation [16], but is also extended to transient operation for healthy and degraded conditions. Finally, a simplified techno economic assessment based on the work of Aretakis *et al.* [17] is carried out for evaluating the effects that the accuracy of our method have on the cost of gas turbine maintenance when the compressor is degrading.

2. Methodology

Axial compressor performance maps are used in the gas turbine thermodynamic models for estimation of key component parameters such as the pressure ratio π_c, the corrected mass flow rate $m_c = \left(\frac{\dot{m}_c \times \sqrt{T_2}}{p_2}\right)$ and the isentropic efficiency η_c at several corrected rotational speeds N. A typical compressor map available from the literature [18] has been digitized and reproduced as shown in Fig. 1. Generating compressor maps for low speed regions, that is below 50% of the corrected rotational speed, is another research topic that has been addressed by other researchers [6], [19] and is beyond the scope of this study.

The objective of map generation approaches is to determine mathematical expressions that could accurately capture the shape of the map. This is performed by relating the corrected mass flow rate m_c and the isentropic efficiency η_c with the pressure ratio π_c and the corrected rotational speed N, i.e. $m_c = f(\pi_c, N)$ and $\eta_c = g(m_c, N)$. Another way of expressing the efficiency $\eta_c = h(\pi_c, N)$ is by expressing it as a function of the pressure ratio π_c, which is beneficial for high rotational speed lines that are almost vertical. A detailed description of our proposed method follows in the next subsections.

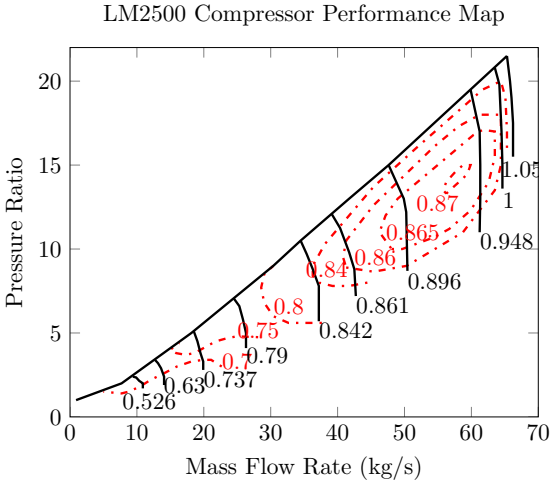

Figure 1: Compressor performance map as reproduced from [18].

2.1. Map Fitting

The process of map fitting commences with a reference map that is available either from the open literature or constructed from the operational data. Having the reference compressor map, the objective is to fit the available data with a single mathematical expression, which should be of the same form for every speed line. The accuracy of the fitting procedure depends on several factors, such as the complexity of the mathematical model chosen, the quality of the data, the threshold of the tolerance criterion and the objective function that is used in the optimization, if any. Several maps from the literature have been used to test the validity of the proposed method but due to space limitations in this work we will only present the accuracy of the method as it is applied to the compressor map shown in Fig. 1. After an extensive review of several methods (polynomials, neural networks [2],[9], etc.) for representing the pressure ratio π_c and the efficiency η_c as a function of m_c and N, the most mathematically robust approach is determined where each line belongs to an elliptic curve. The equation, adjusted for the π_c versus m_c map, is given by

$$\left(\frac{m_{c_0} - x_0}{a_{\pi_c}}\right)^2 + \left(\frac{\pi_{c_0} - y_0}{b_{\pi_c}}\right)^2 = 1 \tag{1}$$

where a_{π_c} and b_{π_c} denote the semi-major and the semi-minor axes of the ellipse, respectively. In addition m_{c_0} and π_{c_0} denote the corrected mass flow rate and the pressure ratio when the ellipse is fixed at (x_0, y_0), which represents the center coordinates of the ellipse, respectively. Taking into consideration that each ellipse is free to rotate, at an angular value of θ_{π_c}, the new coordinates of the ellipse (m_c, π_c) are now given by

$$m_c = m_{c_0}\cos(\theta_{\pi_c}) - \pi_{c_0}\sin(\theta_{\pi_c}) \tag{2}$$

$$\pi_c = m_{c_0} \sin(\theta_{\pi_c}) + \pi_{c_0} \cos(\theta_{\pi_c}) \tag{3}$$

Similarly for the efficiency the governing equation is given by

$$\left(\frac{m_{c_0} - x_0}{a_{\eta_c}}\right)^2 + \left(\frac{\eta_{c_0} - y_0}{b_{\eta_c}}\right)^2 = 1 \tag{4}$$

where a_{η_c} and b_{η_c} denote the semi-minor and the semi-major axes of the ellipse, respectively, and m_{c_0} and η_{c_0} denote the corrected mass flow rate and the efficiency. Once again, rotating the ellipse at an angle of θ_{η_c} yields the compressor's isentropic efficiency η_c as

$$\eta_c = m_{c_0} \sin(\theta_{\eta_c}) + \eta_{c_0} \cos(\theta_{\eta_c}) \tag{5}$$

where eq. (2) is used to determine m_c since the range of the corrected mass flow is identical for both π_c vs. m_c and η_c vs. m_c maps.

The start and the end of the map generated for each speed line are limited according to the variation of each coefficient with respect to the corrected rotational speed N. The distribution of the points at which the surge occurs $\pi_{c_{surge}}$ is expressed as a 2^{nd} order polynomial function of the corrected rotational speed N, as follows:

$$\pi_{c_{surge_i}} = a{N_i}^2 + bN_i + c \tag{6}$$

where a, b, c are the coefficients of the equation and i denotes the corresponding speed line of the surge point $\pi_{c_{surge}}$. Assuming a constant surge margin sm of 20%, the maximum pressure ratio $\pi_{c_{max}}$ of each speed line is then given by:

$$\pi_{c_{max_i}} = \left(\frac{\pi_{c_{surge_i}}}{(1 + sm)}\right) \tag{7}$$

This surge limiter prevents the speed lines from exceeding their corresponding maximum pressure ratio.

Three approaches of varying complexities have been proposed for fitting the π_c versus m_c map data with the following assumptions on the ellipses, namely

Approach 1. Center at $(0, 0)$ and no axes rotation,

Approach 2. Center at $(0, 0)$ and rotation of the axes at an angle of θ,

Approach 3. Center at (x_0, y_0) and rotation of the axes at an angle of θ.

Similar approaches are considered for the η_c versus m_c map apart from the first one, where x_0 is assumed to be the mid point of each curve as follows:

Approach 1. Center at $(x_0, 0)$ and no axes rotation.

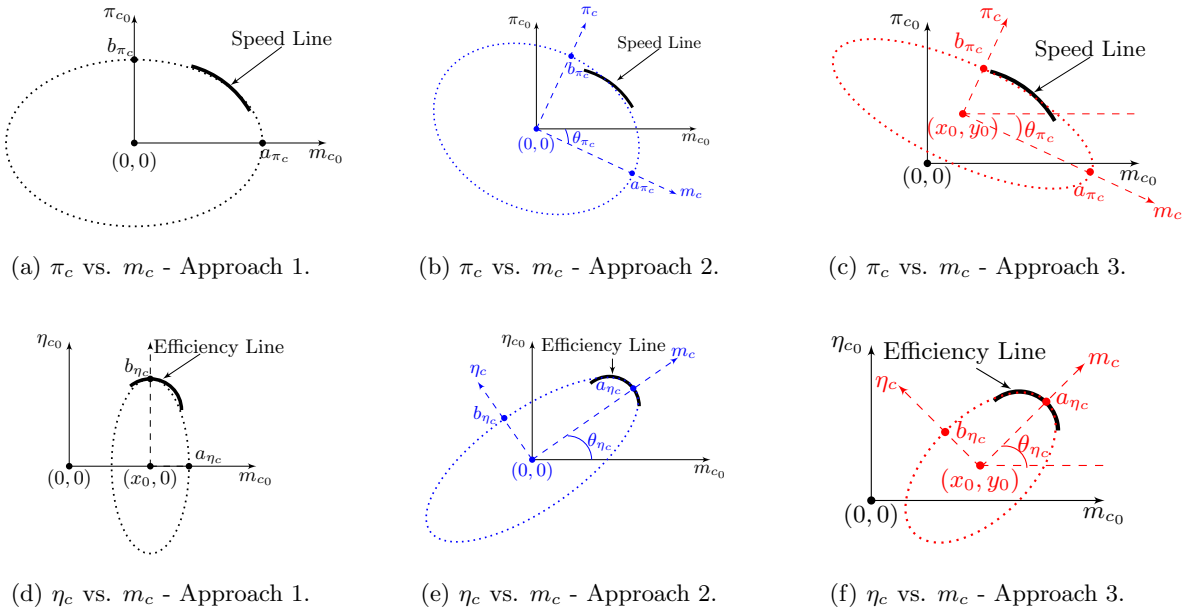

(a) π_c vs. m_c - Approach 1. (b) π_c vs. m_c - Approach 2. (c) π_c vs. m_c - Approach 3.

(d) η_c vs. m_c - Approach 1. (e) η_c vs. m_c - Approach 2. (f) η_c vs. m_c - Approach 3.

Figure 2: Elliptical curve parameters for various fitting approaches.

Approach 2. Center at $(0, 0)$ and rotation of the axes at an angle of θ,

Approach 3. Center at (x_0, y_0) and rotation of the axes at an angle of θ.

A graphical illustration of the suggested elliptical curve fitting approaches along with the important parameters of eqs. (1)-(5) is shown in Fig. 2. Furthermore, a family of the compressor map fitting approaches as suggested by Gholamrezaei and K. Ghorbanian [9], and Yu *et al.* [2] are implemented according to the same objectives. The fitting methods employed here are the GRNN approach with constant and variable spreads σ [9] and a typical BPNN method [2]. The GRNN approach [9] and the BPNN method [2] have been tested by implementing the Matlab's GRNN functions and the NN toolbox [21], respectively. The value of each coefficient for the Approaches 1, 2 and 3 has been determined by integrating the above elliptical functions in one of the Matlab's minimization algorithms (specifically the [fminsearch] [21]). The initial conditions for these coefficients did not require any expert knowledge and could be easily set based on the elliptical curve properties as shown in Fig. 2. The application of the proposed and available methods for the selected map is shown in Fig. 3.

It is observed from Figs. 3a and 3b that the Approach 1 yields similar results as in the GRNN method with constant spread σ. When approaching the high corrected rotational speed N region, the accuracy of both methods decreases and they are not accurately capturing the curvature of each speed line. In the second group of fitting approaches, as shown in Figs. 3c and 3d, Approach 2 is more accurate than Approach 1 and the BPNN fitting method. Once again, at the high rotational speed N region the BPNN performance is not as accurate; nevertheless it is more accurate than Approach 1 and GRNN with fixed spread.

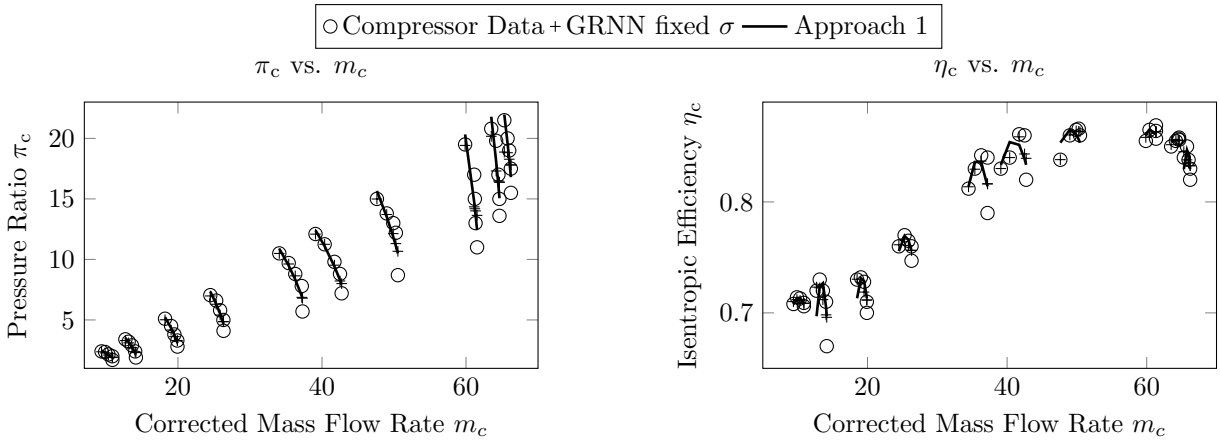

(a) π_c-Fitting (Approach 1 and GRNN fixed σ).

(b) η_c-Fitting (Approach 1 and GRNN fixed σ).

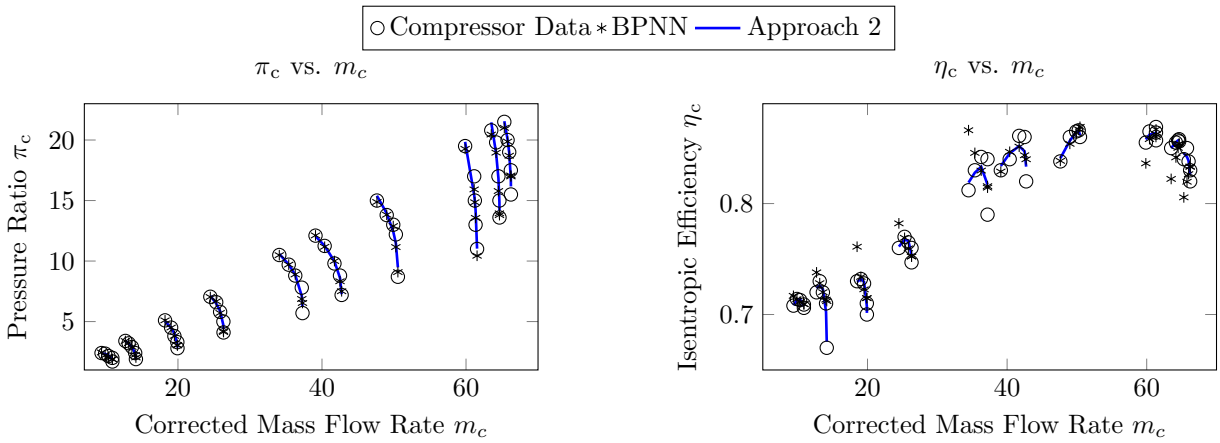

(c) π_c-Fitting (Approach 2 and BPNN).

(d) η_c-Fitting (Approach 2 and BPNN).

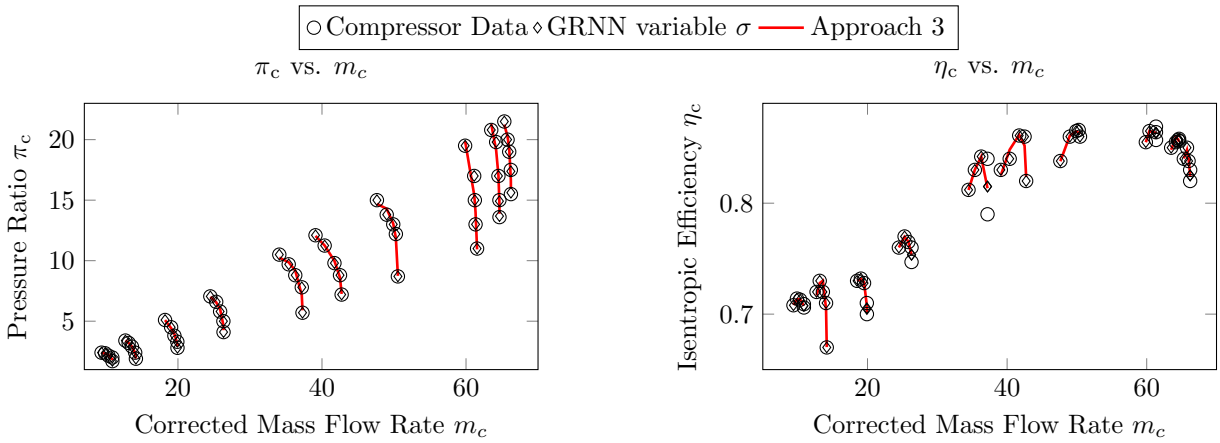

(e) π_c-Fitting (Approach 3 and GRNN variable σ).

(f) η_c-Fitting (Approach 3 and GRNN variable σ).

Figure 3: Compressor performance map fitting methods.

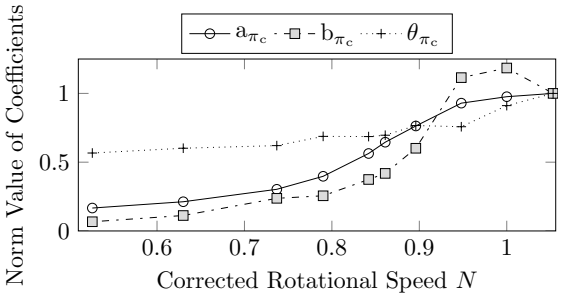

Figure 4: Variation of the proposed map fitting coefficients as a function of the corrected speed N for the π_c versus m_c map.

It is evident from the final group of fitting approaches that are shown in Figs. 3e and 3f, that Approach 3 provides a very good agreement with the compressor map data; as does the GRNN method with variable spread. We are now in a position to evaluate the above proposed approaches in terms of their computational cost and fitting performance given that they have different complexities. The common parameters of each ellipse in all the proposed approaches are a and b. In addition, the angles θ_{η_c} and θ_{π_c} of the rotated ellipses are employed in both the Approaches 2 and 3. The third approach has also the center coordinate parameters (x_0, y_0) and Approach 1 has an additional parameter x_0 for the efficiency map. The only important parameter to be computed in both GRNN methods is the spread or the smoothing parameter σ.

All the above parameters or coefficients should be expressed as functions of the corrected rotational speed N. This process results in a number of sub-coefficients depending on the type of the function. The propagation of the coefficients with respect to N should be captured by smooth and simple functions that will not give rise to ill-conditioned extrapolation affecting the accuracy of the targeted optimization solution. Each coefficient of the suggested elliptical approach is now expressed as a polynomial function of the corrected rotational speed in the generic form as

$$g(N) = g_1 N^i + \cdots + g_i N + g_{i+1} \tag{8}$$

where g denotes as one of map coefficients and i denotes the order of the polynomial function. For instance, in the second approach, the coefficient a_{π_c} is now expressed as

$$a_{\pi_c}(N) = a_{\pi_{c_1}} N^3 + a_{\pi_{c_2}} N^2 + a_{\pi_{c_3}} N + a_{\pi_{c_4}} \tag{9}$$

which is a 3^{rd} order polynomial with a total number of 4 sub-coefficients. In Approach 2 where the coefficients for the pressure map $(a_{\pi_c}, b_{\pi_c}, \theta_{\pi_c})$ are expressed as a function of the speed, as shown in Fig. 4, this results in 13 sub-coefficients for the π_c versus m_c map.

The above process is performed for all the three proposed fitting approaches using the Matlab's curve fitting toolbox. The total number of the sub-coefficients for each proposed approach along with the fitting

errors of the available methods are tabulated in Table 1. For the GRNN method with a constant spread this parameter can be expressed as a linear function of the corrected rotational speed N with only two sub-coefficients, i.e. $\sigma = \sigma_1 N + \sigma_2$. The qualitative evaluation and comparison of the above compressor map

Table 1: Evaluation of various compressor map fitting methods.

Method	Coefficient	Coefficient as $f(N)$	Sub-coefficients	No of Sub-coef.	Fit Error m_c, η_c (%)
App.1 [13]	a_{π_c}, b_{π_c}, a_{η_c}, b_{η_c}, $x_{0_{\eta_c}}$	Polynomial	$a_{\pi_{c_{1\ldots4}}}$, $b_{\pi_{c_{1\ldots4}}}$, $a_{\eta_{c_{1\ldots4}}}$, $b_{\eta_{c_{1\ldots4}}}$, $x_{0\eta_{c_{1\ldots4}}}$	20	6.5, 0.89
App. 2	a_{π_c}, b_{π_c}, θ_{π_c}, a_{η_c}, b_{η_c}, θ_{η_c}	Polynomial	$a_{\pi_{c_{1\ldots4}}}$, $b_{\pi_{c_{1\ldots5}}}$, $\theta_{\pi_{c_{1\ldots4}}}$, $a_{\eta_{c_{1\ldots3}}}$, $b_{\eta_{c_{1\ldots4}}}$, $\theta_{\eta_{c_{1\ldots3}}}$	23	2.9, 0.54
App. 3	a_{π_c}, b_{π_c}, θ_{π_c}, $x_{0_{\pi_c}}$, $y_{0_{\pi_c}}$, a_{η_c}, b_{η_c}, θ_{η_c}, $x_{0_{\eta_c}}$, $y_{0_{\eta_c}}$	Polynomial & Splines	$a_{\pi_{c_{1\ldots8}}}$, $b_{\pi_{c_{1\ldots9}}}$, $\theta_{\pi_{c_{1\ldots10}}}$, $x_{0\pi_{c_{1\ldots13}}}$, $y_{0\pi_{c_{1\ldots9}}}$, $a_{\eta_{c_{1\ldots10}}}$, $b_{\eta_{c_{1\ldots8}}}$, $\theta_{\eta_{c_{1\ldots12}}}$, $x_{0\eta_{c_{1\ldots14}}}$, $y_{0\eta_{c_{1\ldots7}}}$	100	2.2, 0.41
BPNN [2]	-	-	-	-	3.8, 1.41
GRNN constant σ [9]	σ	Linear	$\sigma_{1\ldots2}$	2	6.5, 0.71
GRNN variable σ [9]	σ	-	-	-	0.5, 0.24

fitting methods highlight several trade-offs among their performance, robustness and further implementation in gas turbine models. Generally, the GRNN with fixed spread parameter is a good candidate along with the Approach 1, since they are able to extrapolate data in a compressor map, but both suffer in terms of accuracy. Approach 3 yields the most accurate results among the proposed elliptical fitting approaches due to the fact that there is freedom in changing the center coordinates of the ellipses and simultaneously rotating them. The distribution of the Approach 3 coefficients, as a function of N, is highly nonlinear and only high order polynomials and spline curves are capable of capturing effectively this nonlinear distribution. This results in the use of 100 sub-coefficients for the Approach 3 as opposed to 23 that are required for the Approach 2 although their differences are not significant in both the pressure ratio and the efficiency maps.

Approach 2 has a fitting error of 2.9% for m_c which may be considered high to allow for an accurate

prediction given that for diagnostic purposes one examines faults greater than 1%. However, this fitting error refers to the accumulated deviation from all the points of the reference map. This implies that the average fitting error in Approach 2 for m_c is 0.044% corresponding to each one of the 50 data points. The GRNN with variable spread provides excellent results, however it has the same disadvantage as Approach 3 in terms of its implementation in a gas turbine model, since the distribution of the spread parameter as a function of the speed is highly nonlinear to allow for reliable extrapolation. The excessive parameters corresponding to the GRNN with the variable spread has motivated the development of the rotated GRNN (RGRNN) and MLP approaches as presented in [9]. While accuracy is improved by the latter methods, the RGRNN is limited to represent compressor curves for which data are available. On the other hand, further implementation of the MLP approach in a dynamic adaptive engine model for performance prediction and diagnostics remains to be investigated.

The above comparison is made in order to emphasize that although certain methods will always, independent of the map shape, outperform others in fitting the compressor map data, this goal is not the only measure for a successful gas turbine performance prediction and diagnostic scheme. The well-conditioned interpolation, extrapolation and the ability of the map fitting algorithms to account for the degradation factors are far more important and crucial than their absolute accuracy that is expressed in terms of the fitting error criterion.

Therefore, we have concluded that Approach 2 is selected to be implemented for the engine performance prediction by its integration in a gas turbine model. This decision is justified by the fact that Approach 2 yields a good balance between the accuracy that is obtained and the complexity of the mathematical expressions capturing the variations of each coefficient with respect to the speed. The analytical methodology enables one to formally control the compressor map shape in a nonlinear manner, so that the corresponding map generation method can replace simple lookup tables and/or externally linear-scaled maps in an engine model. Another advantage of our proposed fitting method, due to the analytical nature of the expressions employed for representing an ellipse, is the fact that initial values of the coefficients (a, b, θ) can be selected without any empirical knowledge of the desired maps.

2.2. Gas Turbine Engine Model

The proposed compressor map fitting method is now integrated into a dynamic model of a two shaft industrial gas turbine that is developed in Matlab/Simulink environment and validated with PROOSIS [14]. The engine model that is developed consists of a compressor, a combustor, a compressor turbine and a power turbine as shown in Fig. 5. The components are represented by a set of suitable component maps from PROOSIS, although the compressor map that is used is the one shown Fig. 1.

The engine simulations performed consist of two modes, the steady state and the transient. Steady state simulations are performed for a scheduled variation of the rotational speed N and through an iterative

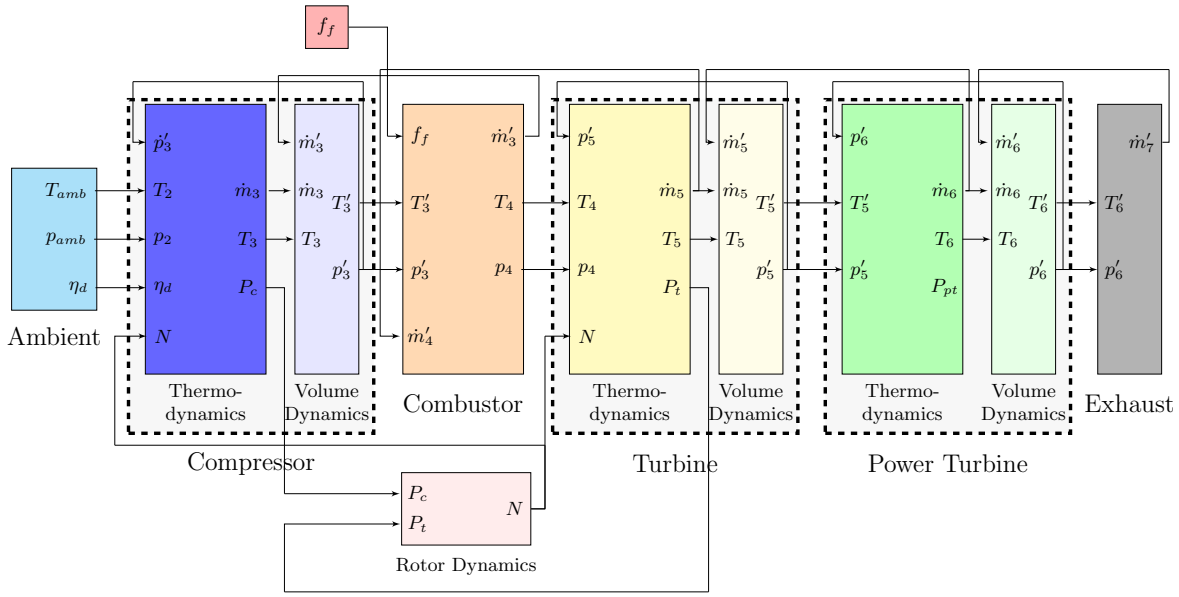

Figure 5: Engine model layout in Simulink (for definition of the variables refer to the Nomenclature section).

method, that selects key component parameters (i.e. mass flow rate $\dot{m}$, Turbine Entry Temperature (TET), etc.) for satisfying the mass flow and the work compatibility laws, where the model converges to the steady state condition. From the converged steady state condition, the values of temperatures at the compressor, combustor, compressor turbine and the power turbine exits, namely, T_3, T_4, T_5, T_6, are passed onto the transient model's plenum volumes as initial conditions.

The transient simulation, based on the Inter Component Volume (ICV) method [20], commences from the last known converged steady state condition of the model with the variation of the control vector which is the fuel flow f_f. As can be observed from the engine layout shown in Fig. 5 plenums are introduced between various components to account for all the flow imbalances to occur in these volumes. These mass imbalances are used to evaluate the rate of the pressure increase to the engine and hence calculate the values of the pressures at the compressor, turbine and the power turbine plenum exits, namely, p'_3, p'_5, p'_6. The difference between the power required by the compressor P_c and the power extracted from the turbine P_t at any given time instant yields an estimate of the rotor acceleration, and hence the rotor speed N. The process is repeated for the next time interval until the end of the simulation time is reached. The developed engine model in the Simulink, an object oriented environment, can be easily adapted to any kind of gas turbine configuration. A detailed description of the model used for this application can be found in our earlier work in [15].

2.3. Model Adaptation

Model performance adaptation is concerned with the inverse performance analysis where engine component characteristics are tuned until they reproduce the measured engine behavior at the same environmental conditions and throttle setting. Generally the engine behavior, assuming no measurement noise or bias, is expressed as follows:

$$\mathbf{Y} = f(\mathbf{X}, \mathbf{u}) \tag{10}$$

where $\mathbf{Y}$ denotes the engine performance vector consisting of the measurements such as the pressure and the temperature at different engine gas path locations, namely $\mathbf{Y} = [p, T]$. The component characteristic vector $\mathbf{X}$ includes non-measurable quantities such as the corrected mass flow and the efficiency, namely $\mathbf{X} = [m_c, \eta_c]$ and $\mathbf{u}$ denotes the ambient and the operating conditions vector consisting of ambient conditions and a parameter called *handle* of the engine model which acts as input to the model for engine performance simulations, namely $\mathbf{u} = [p_{amb}, T_{amb}, handle]$. Depending on the simulation approach selected, the *handle* can be either useful power output from the power turbine P_{pt}, TET, corrected rotational speed N or any other quantity.

The measured engine behaviour is represented either by the field data of a service engine or through simulations of a different engine model. For conducting testing of our proposed method, the *reference engine* is an engine model that uses the compressor performance map of Fig. 1. In contrast to the map generation procedure that is employed by the *engine model*, the *reference engine* employs the map of Fig. 1 as simple lookup tables for determining the corrected mass flow rate and the isentropic efficiency of the compressor.

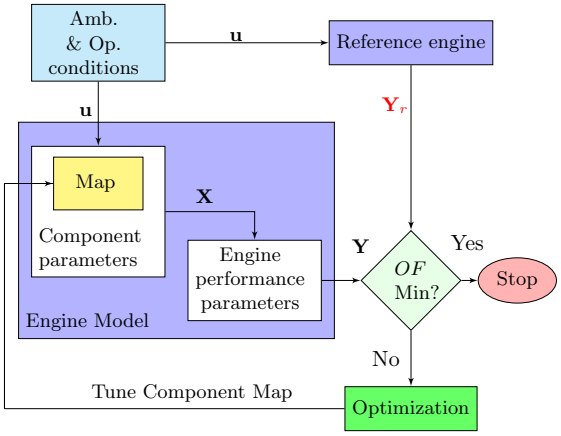

Figure 6: Flow chart of adaptive performance simulation.

The adaptive simulation algorithm that is depicted in Fig. 6 attempts to tune the component characteristics vector $\mathbf{X}$ so that the difference between the performance vector of the *engine model* $\mathbf{Y}$ and the

reference engine $\mathbf{Y}_r$ is minimized. For this study, the difference between the predicted $\mathbf{Y}$ and the observed $\mathbf{Y}_r$ measurements can be evaluated by means of an Objective Function (OF) that is defined as follows:

$$OF = \|\mathbf{A}\|_F = \sqrt{\sum_{i=1}^{q}\sum_{j=1}^{n}|\alpha_{i,j}|^2} \tag{11}$$

$$= \sqrt{\sum_{i=1}^{q}\sum_{j=1}^{n}\left|\frac{\mathbf{Y}_{i,j} - \mathbf{Y}_{r_{i,j}}}{\mathbf{Y}_{r_{i,j}}}\right|^2} \tag{12}$$

where n denotes the total number of operating points corresponding to q number of different corrected rotational speed lines. The Frobenius norm $\|\mathbf{A}\|_F$ of an $m \times n$ matrix A is defined as the sum of the absolute squares of its elements $\alpha_{\mathbf{i,j}}$. The element $\alpha_{\mathbf{i,j}}$ denotes the difference between the predicted $\mathbf{Y}_{i,j}$ and the measurable performance vector $\mathbf{Y}_{r_{i,j}}$, divided by $\mathbf{Y}_{i,j}$. Since the above adaptive performance simulation covers multiple operating points, the objective function was modified to accommodate for such a feature. The number of the measured parameters to be matched depends on the test case itself, however for this work all the measured parameters are used in a single optimization problem.

The criterion OF is minimized by implementing one of the Matlab's built-in nonlinear unconstrained optimization algorithms [fminsearch] [21], which is an implementation of the Nelder Mead algorithm [22]. This algorithm is most effective in exploring the neighborhood of the starting point and converging to a local minimum of OF. However, mathematically multiple solutions might be possible since the algorithm employed here might not always provide the global minimum of OF. This limitation is addressed by initially matching the operating points that are close to the design point of the engine and then moving further away from the design point. Another measure taken to address the former limitation is to set the optimization without any constraints on the sub-coefficients values in order to increase the search space. The last criterion for successful optimization is that convergence of the solution should occur before reaching the maximum number of iterations. The above steps ensure that the solution obtained is the global minimum of the OF.

It should be emphasized that the proposed method assumes the existence of an initial map shape. There is no similarity or closeness requirement between the initial map selected for the *engine model* and the unknown compressor map of the reference test engine. This is supported by the fact that the method is capable of regenerating any shape of the compressor map since the map curves are analytically controlled. The number of the sub-coefficients utilized has to do only with the fidelity by which a compressor map shape is generated and is not related to the number of gas path measurements that are to be matched. The adaptation procedure is now described as follows:

1. Select an initial compressor map from the open literature or any other available source.

2. Scale the map linearly so that the compressor map parameters at 100% of their nominal value $(m_{c_{map}}, \eta_{c_{map}}, \pi_{c_{map}})$ satisfy the design point performance of the reference engine $(m_{c_{des}}, \eta c_{des}, \pi c_{des})$.

3. Fit the elliptical curves to the linear scaled initial map in order to determine the coefficients a_{π_c}, b_{π_c}, θ_{π_c}, a_{η_c}, b_{η_c}, θ_{η_c}.

4. Express the coefficients with respect to the corrected rotational speed N and determine the values of the 23 sub-coefficients. Note that one may choose to match a map shape that is uniformly smooth and not so mathematically challenging as the one shown in Fig. 3 in order to utilize high order polynomials for expressing several map coefficients. This is something that is facilitated by the optimizer since the algorithm has the freedom to assign zero values to the sub-coefficients, and therefore reduce the order of the polynomials.

5. Integrate the map fitting equations along with the sub-coefficients of the initial scaled map in a gas turbine engine model.

6. Utilize the gas path measurements of a reference engine and let the adaptation process tune the sub-coefficients to generate an adapted map for matching all the measurements. Note that before the adaptation process is employed the simulated engine measurements will have significant deviations from those of the reference engine, and in some cases convergence of the engine model might not be possible before invoking the optimization process.

7. The final adapted map is a compressor map that is capable of generating the same results as the gas path measurements available. The generated map is only an approximation to the unknown map since there are many uncertainties such as measurement noise, humidity, etc., that are not accounted for.

Specifically, for the case studies examined in this paper the initial values of the sub-coefficients are determined by the fitting procedure performed earlier to a typical reference compressor map. These are passed onto the compressor map generation procedure as shown in Fig. 7, along with the measured corrected rotational speed N_r, in order to determine the coefficients of the map $(a_{\pi_c}, b_{\pi_c}, \theta_{\pi_c}, a_{\eta_c}, b_{\eta_c}, \theta_{\eta_c})$. Once the coefficients are calculated, the pressure ratio π_{c_r}, which is a known measurable parameter of the reference engine, is used for determining the corrected mass flow m_c by solving eqs. (1), (2) and (3). The corrected mass flow m_c is then used in the same manner as in π_{c_r} to calculate the compressor's isentropic efficiency η_c from eqs. (4), (5).

Both m_c and η_c form the component characteristics vector $\mathbf{X}$ which is then used in the remaining thermodynamic computations of the engine model. The key optimization parameters, such as the number of iterations and the tolerance criterion are specified accordingly. Once the optimization process converges, the new set of sub-coefficients are passed onto the engine model. The developed algorithm can be executed both for external and internal adaptive simulations. In case of internal adaptive simulation, the optimization of sub-coefficients takes place simultaneously with the iterative computation of the compatibility thermodynamic equations of the engine model.

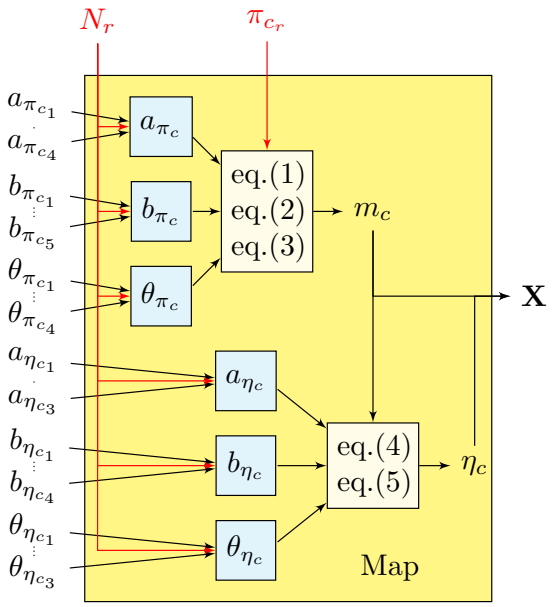

Figure 7: Flow chart of compressor map generation.

The data driven nature of the proposed method implies that the accuracy of the map generated depends on the number of operating points that are available from an engine with an unknown map. However, it should be noted that the generated map is an accurate representation of the unknown map mainly for the region for which the data points are available. This implies that a map can be generated even when a small number of operating points or a set of points distributed in the same speed line are available. The remaining area of the generated map can be considered as a reasonable estimate of the unknown map according to the extrapolation capabilities of the method. The ideal case will be when the targeted operating points cover a wide area of the map. In such a case the generated map is a more accurate representation of the unknown map.

2.4. Adaptive Diagnostics

An additional feature of the model adaptation is that it can be applied not only for performance simulation but also for gas turbine diagnostics. Below we employ the model adaptation scheme for performing engine diagnostics as shown in Fig. 8. The component vector $\mathbf{X}$ consists of mass flow capacity $\Gamma_c = m_c/m_{c_{des}}$ and isentropic efficiency η_c. Compressor degradation of the *reference engine* is represented by the deviation of these parameters from their healthy values, i.e. $\Delta\Gamma_{c_{inj}} = 100(\Gamma_{c_{deg}} - \Gamma_{c_{cl}})/\Gamma_{c_{cl}}$, $\Delta\eta_{c_{inj}} = 100(\eta_{c_{deg}} - \eta_{c_{cl}})/\eta_{c_{cl}}$. The above deviations injected to the *reference engine* form the deviation vector $\Delta\mathbf{X}_{inj}$.

Consequently, the *reference engine* will operate at degraded conditions and will produce a new set of degraded measurable parameters $\mathbf{Y}_{r_{deg}}$. The task of the adaptation scheme in this case is to determine the

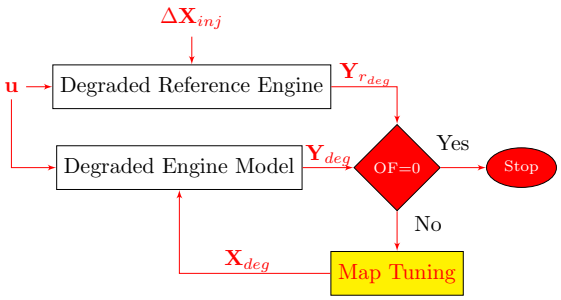

Figure 8: Flow chart of engine model adaptive diagnostics.

rate of the degradation that is injected in the *reference engine*, by tuning the component map of the *engine model* as described earlier. Therefore, the *engine model* matches the targeted degraded measurements of the *reference engine*, by a new set of components parameters that form the degraded vector $\mathbf{X_{deg}}$. The earlier adaptation of the model is in fact a training phase for fault diagnosis since it acts as the reference point for the engine healthy condition. Therefore, the difference between the degraded and the healthy set of component vectors $(\mathbf{X}_{deg}, \mathbf{X}_{cl})$ determines the severity of the degradation

$$\Delta \mathbf{X}_{pred_{i,j}} = 100 \left(\frac{\mathbf{X}_{deg_{i,j}} - \mathbf{X}_{cl_{i,j}}}{\mathbf{X}_{cl_{i,j}}} \right) \tag{13}$$

In order to assess how effective the prediction results are a diagnostic index (DI) is defined as follows

$$DI = 100 \left(\frac{1}{1+\epsilon} \right) \tag{14}$$

where ϵ is the average error in terms of the characteristic vector $\mathbf{X}$ which is the output of the compressor map. In contrast to the gas path analysis (GPA) index used in the GPA methods [23], the one utilized here assesses the effectiveness of the prediction based on the output of the compressor map which forms the characteristic vector $\mathbf{X}$. Consequently, the accuracy by which a map is tuned to meet the degraded gas path measurements is evaluated according to

$$\epsilon = \frac{\sum_{i=1}^{q} \sum_{j=1}^{n} \left(\frac{\Delta \mathbf{X}_{pred_{i,j}} - \Delta \mathbf{X}_{inj_{i,j}}}{\Delta \mathbf{X}_{inj_{i,j}}} \right)}{qn} \tag{15}$$

For multiple operating points, n denotes the total number of points corresponding to q number of different corrected rotational speed lines. The simulation case studies that have been carried out are now described in the following section.

3. Case Study Description

Our proposed adaptation approach is implemented in a dynamic engine model that is developed in the Matlab/Simulink environment and is evaluated and analyzed for the steady state and the transient

conditions. As described earlier, the *reference engine* is a similar model with simple lookup tables whereas the *engine model* utilizes our proposed map generation process. The performance specifications of the *reference engine* are provided in Table 2.

Table 2: Performance specification of the *reference engine*.

Parameter	Value	Units
Power	3.4	MW
Pressure ratio	10.8	
Thermal efficiency	38	%
Exhaust flow rate	34	kg/s

One of the prerequisites for successful model adaptation is that the engine measurable parameters are directly influenced by the component characteristic parameters to be adapted, otherwise non-physical deviations may appear on the component parameters which are not the cause of the initial difference between the predicted model and the measured values. Our primary objective of presenting the case studies is to evaluate the achievable accuracy improvement of our proposed method that incorporates the compressor map tuning and takes into consideration the above pre-requisite. Therefore, the selection of the inlet and the outlet measurements of the compressor are well justified. The list of the selected measurable parameters for conducting the adaptive performance simulations is given in Table 3. The nominal operating point that is chosen as the model design point for this configuration is set at 3.4 MW with the shaft corrected rotational speed N set as the *handle* of the engine.

Table 3: Engine performance measurable parameters.

Symbol	Parameter	Units
p_2	Compressor Inlet Pressure	Pa
T_2	Compressor Inlet Temperature	K
p_3	Compressor Discharge Pressure	Pa
T_3	Compressor Discharge Temperature	K
N_{act}	Shaft Rotational Speed	rpm

Four case studies are conducted. The target measurements in the first case study are the *deck data* that represent the off-design steady state performance of the *reference engine*, when the corrected rotational speed N is reduced from 100% to 55% of its nominal value, and with the selected compressor map implemented

as a lookup table.

The second case study focuses on the performance of the proposed adaptation method when the *deck data* are the outcome of the transient performance of the *reference engine*. The effect that the initial map shape has on the accuracy of the proposed method is also assessed. This is accomplished by using a different initial compressor map shape than the one in Fig. 1, and is available from the PROOSIS gas turbine simulation software [14]. Once again, the initial map seen in Figs. 9 and 10, is used for fitting elliptical curves and determining the values of the sub-coefficients. Based on this map the proposed method is integrated into an additional engine model which is tested in transient conditions.

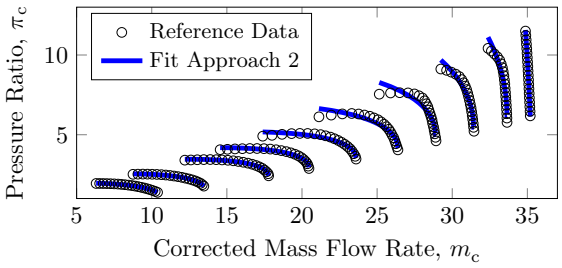

Figure 9: π_c vs. m_c map from PROOSIS [14]

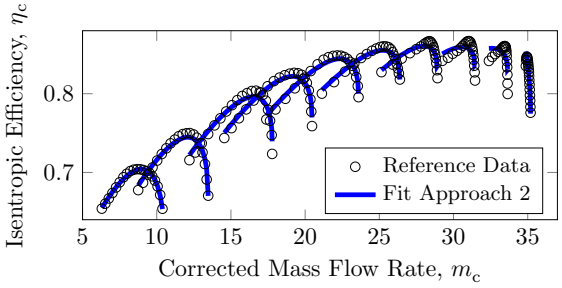

Figure 10: η_c vs. m_c map from PROOSIS [14]

In the third case study the goal of the *engine model* is to match a set of *reference engine* measurements when degradation is injected in the compressor of the latter. Therefore, the method's prediction capability is not only evaluated for improving the performance simulation of the model but also for estimating the severity of the degradation that is injected in the *reference engine*.

In addition, a typical Linear Scaling (LS) method as suggested by Kong *et al.* [3] and the Non Linear Scaling (NLS) method recently developed by Li *et al.* [4] have both been adopted and tested for facilitating their comparison with the proposed method. Both existing methods are integrated in a similar engine model based on the compressor map shape of Fig. 1. In terms of the optimization, both existing methods employed the Matlab [fminsearch] [21] algorithm and not the GA optimization scheme that the authors of [3], [4] have implemented in their work. This is done intentionally since uncertainty or improved accuracy

that is provided by different optimization schemes should be filtered out in order to focus purely on the capability of each method to modify the compressor map shape, and therefore ensure that the comparisons between them are more realistic.

For the transient mode cases, the fuel flow rate varies according to the fuel flow command schedule and the engine is decelerated and accelerated as described in Sections 4.2 and 4.3. The adaptation case study

Table 4: Simulation parameters of the adaptation case studies.

Case	Mode	Points	Iterations	Fun. Eval.	Error Tol.
1	Steady	9	10^3	2×10^3	10^{-8}
2	Transient	100	10^4	2×10^4	10^{-14}
3	Transient	60	10^4	2×10^4	10^{-14}

parameters are provided in Table 4, where the number of maximum iterations range from 10^3 to 10^4 with the function evaluations being twice these values and the error tolerance ranges from 10^{-8} to 10^{-14}. The function evaluations refer to the number of times that the optimization algorithm is allowed to evaluate the objective function, whereas the iterations refer to how many times this algorithm is allowed to be performed.

The fourth case study is a techno economic assessment of each adaptation method and their associated cost in terms of the maintenance if adopted in a thermal power plant for performance estimation of the compressor degradation.

4. Results and Discussion

Our proposed adaptation approach is tested for both the steady state and the transient modes of the healthy and degraded conditions. The results for each case study are presented and discussed in the following subsections.

4.1. Steady State Case Study

4.1.1. Case 1

The objective of the first case study is to evaluate the accuracy of our proposed adaptation method and compare it with the LS and NLS methods for a wide range of off-design steady state operations. Having the corrected rotational speed as the *handle*, the *engine model* is able to match the *deck data* of the *reference engine* at a variable level of accuracy for each method as seen in Fig. 11. It is concluded from Fig. 11 that

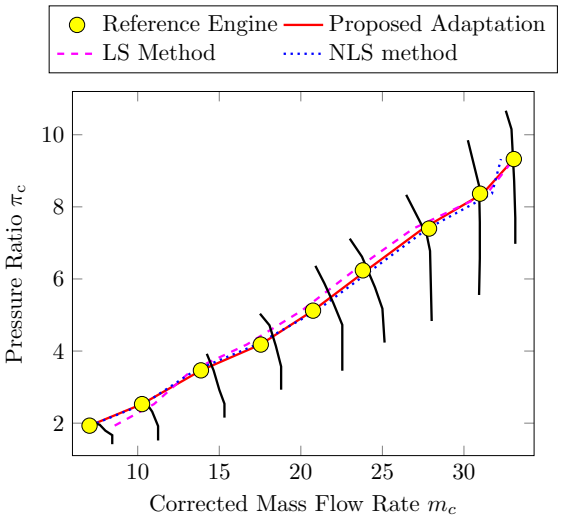

Figure 11: Steady state operating line as predicted by various adaptation methods.

the proposed method is very accurate. The NLS method has a similar accuracy with that of the proposed method, but this is not the case for the LS method. The former observation is more evident from Fig. 12.

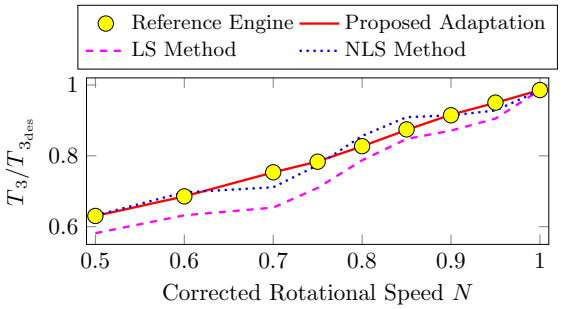

Figure 12: Normalized to design conditions compressor discharge temperature as predicted by various adaptation methods for the steady state.

The *engine model* prediction error for each method is shown in Fig. 13. The engine model prediction error for the LS method is increasing when the operating point is far away from the design conditions. This is due to the fact that a major assumption for a successful adaptation in this method is that the compressor map to be tuned should be of very similar shape to that of the one used by the *reference engine*. On the other hand, the accuracy of the NLS method is distributed in a balanced way, and any deviations are due to the specific shape of the *reference engine* map as seen in Fig. 1 and the wide range for which that adaptation is pursued.

The compressor discharge pressure p_3 and the temperature T_3 for the engine model show a maximum error in the range of -2% to 2% for the proposed method. On the other hand, the maximum engine model errors for the LS and the NLS methods are in the ranges of -10% to 10% and -5% to 4%, respectively. Moreover, the

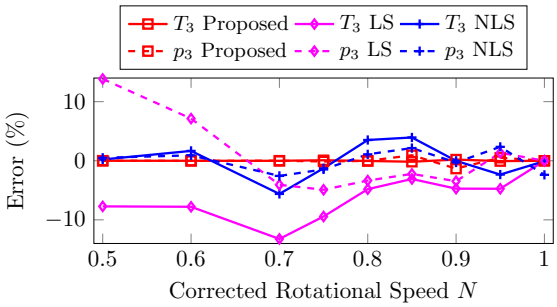

Figure 13: Measurable parameters error of various adaptation methods for the steady state.

engine model that utilizes the proposed adaptation method has an average error in T_3 which is equivalent to 0.05K, whereas for the linear and the nonlinear scaling methods this is 15K and 2K, respectively. Figure 14 shows the margin by which each one of the 23 sub-coefficients that control the compressor map generation process proposed are modified in order to match the target measurable parameters. The normalized values as shown in Fig. 14 simply refer to the ratio between the tuned and the initial sub-coefficients.

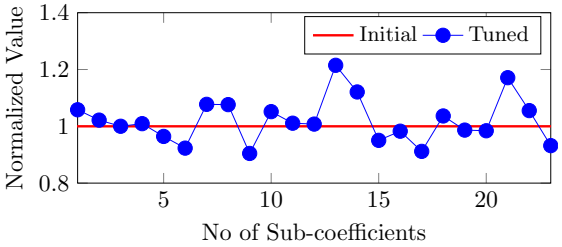

Figure 14: Initial and tuned map sub-coefficients for the proposed adaptation method.

Another key aspect of the entire optimization process, which involves the tuning of the sub-coefficients, is its rapid convergence. For this case study where 800 iterations and a total 2000 function evaluations were required the computation time when performed in a modern PC equipped with Intel's i5 quad-core processors and 4GB of RAM memory was only 0.23 sec. The computation time for the LS and the NLS methods was 0.1 sec and 0.4 sec, respectively.

4.2. Transient Mode Case Studies

4.2.1. Case 2

The objective of the second case study is to evaluate the accuracy of our proposed adaptation method in transient conditions and evaluate how this may be affected by the initial map shape selected. Therefore, in this case study an additional model (Model II) is employed in which the compressor map sub-coefficients have been determined by fitting the data of another compressor map from PROOSIS, as described earlier

in Section 3. The initial *engine model* where the compressor map generation was based on the map shown in Fig. 1 is going to be referred to as Model I for this case study.

In contrast to the previous steady state case where the operating range was wide, in this transient case we are focusing on a much narrower range, i.e. from 100% to 90% of the nominal value of the rotational speed N. The reason for this selection is firstly due to the fact that the majority of industrial gas turbines used for power generation spend most of their lifetime within this operating range, and secondly because we want to compare different adaptation methods in a operating region where their accuracy seem to be of similar magnitude as shown in Fig. 13.

It should be emphasized that the transient case sheds more light on the accuracy by which each adaptation method reconstructs a compressor map shape. Note that by default the acceleration and deceleration trajectories of the engine access a larger proportion of the map shape itself in comparison with the steady state operating points which are within a single running line of the map. The fuel flow rate for this case is scheduled accordingly and the fuel flow command is shown in Fig. 15. Simulation results for the specified fuel

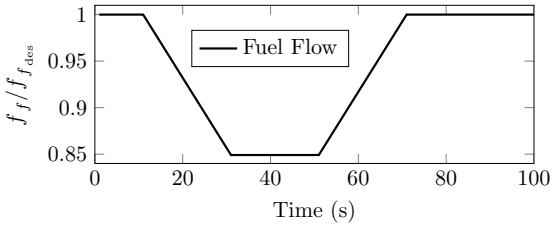

Figure 15: Fuel flow schedule for the transient response.

flow schedule of the *reference engine* and the engine models after employing different adaptation methods are shown in Figs. 16 and 17.

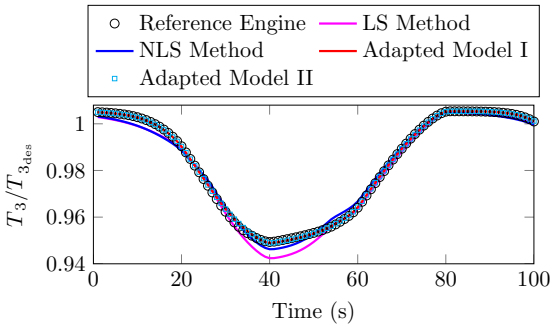

Figure 16: Normalized to design conditions compressor discharge temperature as predicted by various adaptation methods during transient response.

As observed from Fig. 16, both Model I and Model II employing the proposed adaptation are in excellent agreement with the *reference engine*. It should be noted that although Model I and Model II are based on

a different compressor map their prediction is identical. This is something expected for a couple of reasons that is going to be described below. The difference between the two scaling methods [3], [4] is not significant since the operating range is small and both have matched the targeted measurements with an appropriate level of accurately.

The proposed adaptation is capable of following the transient response as seen from the acceleration and deceleration trajectories that are shown in Fig. 17 more accurately than the other scaling methods. A closer look at Fig. 17 reveals the effects that the different compressor map shapes employed in each Model I and Model II have on the accuracy of the prediction before the adaptation is employed. It becomes clear that Model II underperforms significantly in comparison with Model I before adaptation. This has to do solely with the difference in the initial compressor map shape selected, as the one of Model I is similar to the one used by the *reference engine*. This difference has been minimized by employing the adaptation procedure.

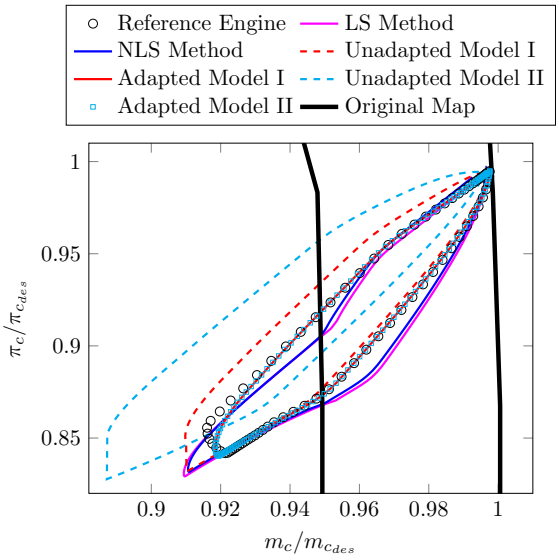

Figure 17: Transient trajectories on the compressor characteristic map for various adaptation methods.

The unconstrained nature of the optimization algorithm employed and the method by which the compressor map curves are fitted are the most important factors in matching any compressor map shape, independent of the initial map selected. The margin by which the 23 sub-coefficients of Model II have to be tuned to match the *reference engine* data is larger that the one of Model I, as seen from Fig. 18. Furthermore, the values of the sub-coefficients after adaptation are the same for both Models I & II. This confirms the fact that the [fminsearch] algorithm [21] was capable of converging to the same solution even if the initial values of the 23 sub-coefficients employed in Models I & II were different. It can be concluded that the proposed method, independent of the initial map shape, can successfully control the position, distribution, spacing and curvature of the elliptical curves passing through multiple data points. Hence compressor map shapes

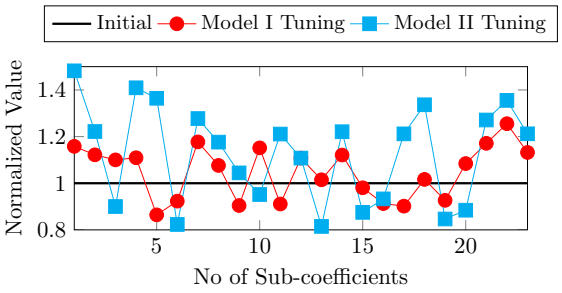

Figure 18: Initial and tuned map sub-coefficients for the adapted engine Models I & II.

can be effectively generated.

In terms of the optimization process where a total of 100 discrete operating points were used for this case the process converged after 5000 iterations, 20000 function evaluations with the elapsed CPU time of 0.8 sec for the Model I. The difference in computation performance between Model I and Model II was negligible, as Model II performed 6400 iterations to reach the same tolerance criteria at an elapsed CPU time of 1.1 sec. On the other hand, the elapsed CPU time for the LS and NLS methods was 0.2 sec and 2.1 sec, respectively.

The prediction error of each method for the transient case study is shown in Fig. 19. The prediction error in the compressor discharge pressure p_3 and the temperature T_3 for the proposed adaptation are in the range of -0.3% to 0.1%, as opposed to the LS and NLS methods that are both within the range of -1.2% to 1.1%.

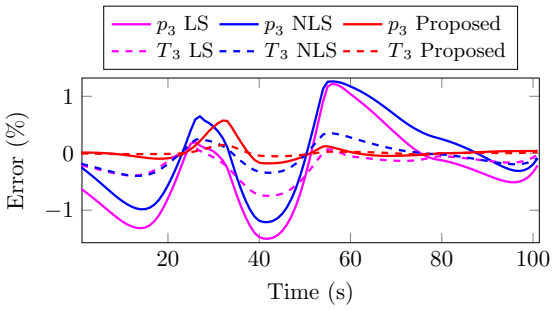

Figure 19: Measurable parameters error of various adaptation methods during transient response.

For instance, the adapted Models I & II have an average error in T_3 which is equivalent to 0.2K, whereas for the scaling method the average error is about 1K. A prediction error of 1% for scaling methods is acceptable in terms of engine performance prediction, but it should be once more noted that the operating range that the adaptation is performed is close to the design point of the engine where both methods perform accurately in principle. In the following subsection the degradations are injected in the *reference engine* so that the capabilities of each adaptation method are tested to their limits.

4.2.2. Case 3

The objective of this case study is to evaluate the capability of our proposed method to predict a component degradation. As described earlier in Section 2.3, the mass flow capacity and efficiency of the *reference engine* compressor are reduced by -5% and -2.5%, respectively. This percentage decrease represents a typical maximum rate of the compressor fouling for a gas turbine that can be partly recovered with off-line washing. Generally, given that steady state data of high quality are difficult to obtain, diagnosing the health of a gas turbine might be based on transient data. Although the former is computationally challenging it should be noted that transient behavior is much more sensitive to the degradation than the steady state. Consequently, transient data can provide a better insight when one is required to perform fault diagnosis and health monitoring during this operational mode.

The fuel flow for the transient maneuver is identical to the one shown in Fig. 15. A total of 60 discrete operating points were used for the adaptation case. The *engine model* after adaptation matches the degraded *reference engine* measurable parameters at a different level of accuracy depending on the method employed. The engine model predictions are in good agreement with the *reference engine* for the degraded conditions as well. The deviations $\Delta\Gamma_c$, $\Delta\eta_c$ used in Figs. 20 and 21 refer to the difference between the predicted and injected component degradation as defined in eq. (13), i.e. $\Delta\Gamma_c = \Delta\Gamma_{c_{pred}} - \Delta\Gamma_{c_{inj}}$. As can be observed, the errors are in the range of -0.2% to 0.2% for the proposed adaptation method. For the LS and NLS methods the errors are in the range of -6.0% to 2.3% and -2.2% to 1.0%, respectively.

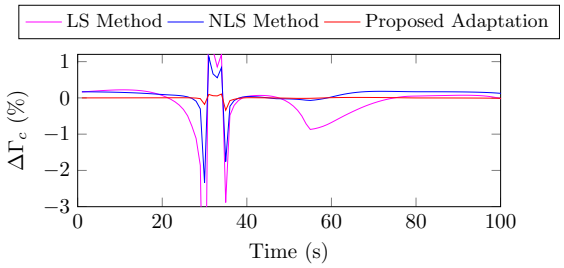

Figure 20: Deviation in mass flow capacity as predicted by various adaptation methods during transient response.

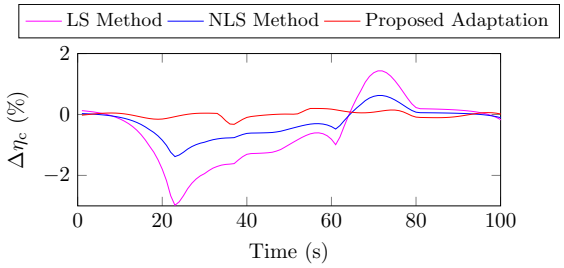

Figure 21: Deviation in compressor isentropic efficiency as predicted by various adaptation methods during transient response.

Table 5: Adaptation results for various case studies (CS).

Approach	Performance			Computation		
	Mean Error (%)	Mean Error (%)	DI (%)	Time (sec)		
	CS 1	CS 2	CS 3	CS 1	CS 2	CS 3
LS	3.0	0.9	67	0.1	0.2	0.18
NLS	1.2	0.8	88	0.4	2.1	1.6
Proposed	0.15	0.1	98	0.23	0.8	0.7

As expected, the error becomes more evident in the transient phase of the operation. Our employed adaptation method predicts the injected degradation with an average error of 0.08% for the mass flow capacity and 0.027% for the isentropic efficiency. On the other hand, the average error for the LS and the NLS methods is 0.6% and 0.2% for the mass flow capacity and 1.3% and 0.7% for the isentropic efficiency, respectively. The diagnostic index for our proposed method is 0.9894, which implies that the diagnosis is 98.94% effective and in comparison with the LS and the NLS methods it is more accurate by 31% and 10%, respectively. The case study results demonstrate the promising prospect of our method when applied for a gas turbine performance diagnosis. The proposed adaptation process converged after 6000 iterations, 20000 function evaluations with an elapsed CPU time of 0.9 sec.

The maximum deviations of -5% in the compressor flow capacity and -2.5% in the isentropic efficiency are selected specifically in order to demonstrate the capability of our proposed approach to a more challenging diagnostic task than considering deviations of -1% and lower. However, it should be noted that the accuracy of our method remains unchanged even for smaller deviations of the component parameters. The results from all case studies (CS) are summarized as shown in Table 5.

4.3. Techno Economic Case Study

4.3.1. Case 4

The primary objective of this case study is to assess the effects that each adaptation method have on the quality of engine performance information that are usually implemented by the gas turbine users for maintenance of a power plant. Generally gas turbine users implement various tools for estimating the health of gas turbine compressor in terms of the mass flow capacity and the efficiency. Depending on the severity of degradation that is predicted by the selected approaches, the plant has to be shut down and an off-line washing is carried out to recover the lost performance of the compressor and the engine.

Although both on-line and off-line washing are performed on gas turbine compressors, the former is not accounted here. The reason is that the off-line washing has a higher impact on both recovering the

compressor fouling and increasing the maintenance cost of the plant. The assumptions that are made for this case study are as follows:

- The time frame for which a gas turbine operation is investigated is 12 months.
- Only the compressor degradation due to the fouling is examined.
- A typical constant rate of -1% drop in the compressor efficiency per month is assumed.
- Off-line washing is performed once the estimated drop in the compressor efficiency is 1%.
- After each off-line washing 95% of the lost compressor efficiency is recovered.
- The gas turbine operates most of the time from 100% down to 90% of the nominal rotational speed N.
- Within the above operating range a small proportion (20%) is considered as transient and the remaining (80%) as steady state.
- A weighted average error is determined to account for the earlier assumption, i.e. $\epsilon_w = 0.8\epsilon_s + 0.2\epsilon_{tr}$, where ϵ_s and ϵ_{tr} denote the average errors for the steady state and transient conditions, respectively.
- The proposed adaptation method in conjunction with the scaling methods are employed.

The number of off-line compressor washings that are suggested by each method is shown in Fig. 22 and is compared with the optimum number of washings that are required by the reference engine when adopting the maintenance strategy as encapsulated by the above assumptions.

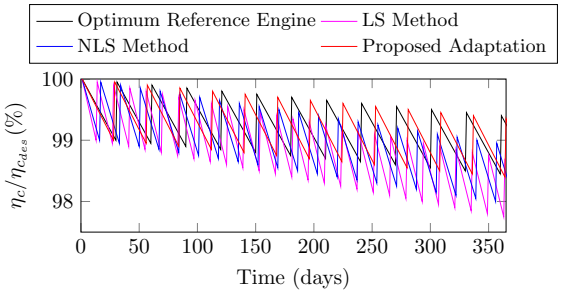

Figure 22: Normalized to design conditions percentage of the compressor efficiency before and after off-line washings as suggested by various adaptation methods. Local troughs represent the estimated drop of the compressor efficiency before performing off-line washing. Peaks represent the recovered compressor efficiency after off-line washing.

It can be observed that the accuracy of the proposed adaptation method suggests 13 off-line washings for a one year period in comparison with the actual compressor degradation of the reference engine that can be optimally recovered with 12 washings only. The total number of washings suggested by the LS and the

NLS methods is 26 and 21, respectively. Although the prediction accuracy of each method that is employed in this case study as shown in Fig 23 is in reasonable levels, their difference increases exponentially when it comes to the techno economics and the cost that each method implies in the maintenance of the power plant.

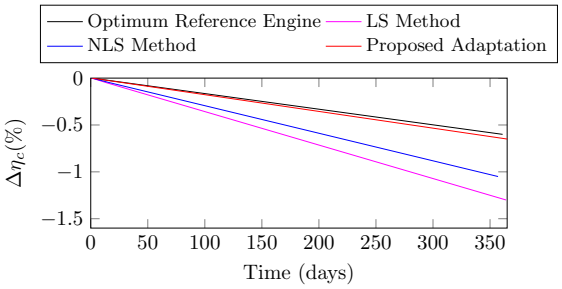

Figure 23: Percentage drop of compressor efficiency as estimated by various adaptation methods when adopting their suggested number of off-line washings.

Let us make a reasonable assumption based on the work of Aretakis *et al.* [17] by considering the extra cost that each method implies in the maintenance of a gas turbine. Let us consider that each off-line washing costs $3000, which is reasonable for an aeroderivative gas turbine, and that the shutdown is about 3 hours. The cost corresponding to each method and its relative cost with respect to the optimum method of the *reference engine* are summarized in Table 6.

Table 6: Cost of off-line compressor washings suggested by various adaptation method.

Approach	Washings	Cost ($)	Cost rel. to the Opt. (%)
Optimum	12	36,000	-
LS Method	28	78,000	216%
NLS Method	21	63,000	175%
Proposed Adaptation	13	39,000	108%

It is evident from Table 6 that the accuracy of our proposed method has the potential to reduce the maintenance cost associated only with off-line compressor washing, by 108% and 67% of the optimum cost in comparison with the existing LS and NLS methods, respectively. In practice, the cost associated with the compressor washing leads to several other associated costs such as shutdown, personnel, etc. that all contribute to the overall maintenance cost of a power plant. However, by using a group of assumptions the effects that the accuracy of various performance adaptation methods have in terms of plant economics are

further amplified.

As far as the practical aspects and limitations of our proposed method is concerned when used in real engines and real fault cases several considerations must be taken into account. Firstly, our proposed method can predict accurately the performance and health of a gas turbine for the range of operation that the initial model is adapted to. Therefore, one should initially adapt the engine model to a wide operating envelope of the engine. Feeding new operating points that belong to speed lines, not previously employed in the adaptation, would only test the extrapolation capability of the map generation method and not the accuracy of the optimization for the diagnostic purposes. The proposed method does not consider variable geometry features such as the variable stator vanes (VSV), and how these affect the geometry of the compressor map generated. This is a limiting factor of our approach when one investigates a wide range of engine operations that utilize variable geometry compressor scheduling by the VSVs.

Data corrections for measurement noise, humidity etc. should be accounted for before utilizing data smoothing. Data averaging for several engine performance measurements, such as the turbine and the power turbine exits, that rely on a set of instrumentation sensors might be employed. This facilitates the establishment of a good quality set of engine operating points to be utilized for the map generation and adaptation. The resulting adapted model forms the benchmark for further diagnostic analysis where deviations of the component parameters will be based upon this. However, one should consider the maintenance activity of an engine from the time of the first adaptation of the engine model up to the time that diagnosis is pursued. Meantime updating and refining the engine model should be performed. This process of continuously updating the engine model will improve the accuracy of the diagnosis significantly.

The desirable features and performance capabilities of the proposed method motivate the inclusion of variable geometry characteristics to the compressor map generation and also the fitting and modelling of turbine maps; tasks that the authors are currently engaged in.

5. Conclusions

In this paper, a novel adaptation method is introduced that aims at improving the accuracy of the gas turbine performance prediction and diagnostics at both the steady state and transient operating conditions. The model coefficients that are obtained from the map generation procedure are optimized through a nonlinear algorithm in order to match the targeted (healthy or degraded) measurements of a reference model with a compressor map that is available in the literature, working at off-design steady and transient conditions. The proposed method deals effectively with the nonlinear behavior of gas turbines away from the nominal operating points by tuning the compressor map shape resulting in accurate compressor degradation diagnostics.

Application of the developed approach to a two shaft industrial gas turbine engine model demonstrates

the following advantages and benefits. In comparison with earlier adaptation methods, our proposed strategy demonstrates the effectiveness that the compressor map has on the prediction accuracy of the engine model. The accuracy of the proposed method is independent of the similarity between the initial map shape selected and the targeted compressor map. The built-in nonlinear optimizer that is employed for this adaptation is effective in minimizing the prediction errors by adapting the compressor maps. The computational time for a typical multi-point steady state adaptation scenario is approximately 0.2 sec for 2000 function evaluations and 750 iterations with an average prediction error of 0.15%. Similarly, corresponding to the transient conditions and for 100 operating points the elapsed CPU time and the prediction error are 0.8 sec and 0.1%, respectively. Our method is applied for predicting a compressor fouling degradation where the results demonstrate a diagnostic accuracy of 99.84% when 60 operating points of the reference engine in the transient mode are considered as the targeted measurements. In addition, the proposed method is capable of reducing the maintenance cost of a plant associated with the compressor washing ranging from 67% up to 108% in comparison with other existing adaptation methods.

Our proposed adaptive performance method is a useful tool for progressively refining an engine model based on multiple sets of reference engine test data at both the steady state and the transient off-design operating conditions. The improved accuracy and efficient computational properties of our method have also demonstrated its potential capabilities for gas turbine diagnostics and reducing the maintenance cost. Therefore, implementation of our proposed method to any gas turbine performance simulation or as a condition monitoring and diagnostic tool could provide a more reliable and accurate information for gas turbine engines, and support the users in making informed decisions on managing efficiently their assets, increasing their availability and reducing their maintenance cost.

Acknowledgements

This publication was made possible by NPRP grant No. 4-195-2-065 from the Qatar National Research Fund (a member of Qatar Foundation). The statements made herein are solely the responsibility of the authors. The authors would also like to acknowledge the constructive comments, and suggestions provided by the anonymous reviewers that greatly improved the quality of the article.

References

[1] I. Templalexis, P. Pilidis, V. Pachidis, P. Kotsiopoulos, Development of a 2-d compressor streamline curvature code, in: ASME Turbo Expo 2006: Power for Land, Sea, and Air, American Society of Mechanical Engineers, 2006, pp. 1005–1014.

[2] Y. Yu, L. Chen, F. Sun, C. Wu, Neural-network based analysis and prediction of a compressor's characteristic performance map, J. Appl. Energy 81 (1) (2007) 48–55.

[3] C. Kong, S. Kho, J. Ki, Component map generation of a gas turbine using genetic algorithms, J. Eng. Gas Turbines Power 128 (1) (2004) 92–96.

[4] Y. G. Li, M. F. A. Ghafir, K. Huang, X. Feng, L. Wang, R. Singh, W. Zhang, Improved multiple point nonlinear genetic algorithm based performance adaptation using least square method, J. Eng. Gas Turbines Power 134 (3) (2012) 031701.

[5] J. Kurzke, How to get component maps for aircraft gas turbine performance calculations, in: Proc. ASME Turbo Expo, 1996.

[6] G. Jones, P. Pilidis, B. Curnock, Extrapolation of compressor characteristics to the low-speed region for sub-idle performance modelling, in: Proc. ASME Turbo Expo, Vol. 2, Amsterdam, Netherlands, 2002, pp. 861–867.

[7] V. Sethi, G. Doulgeris, P. Pilidis, A. Nind, M. Doussinault, P. Cobas, The map fitting tool methodology: gas turbine compressor off-design performance modeling, Journal of Turbomachinery 135 (6) (2013) 061010.

[8] C. Drummond, C. Davison, Capturing the shape variance in gas turbine compressor maps, in: Proc. ASME Turbo Expo, Vol. 1, Orlando, USA, 2009.

[9] K. Ghorbanian, M. Gholamrezaei, An artificial neural network approach to compressor performance prediction, J. Appl. Energy 86 (7) (2009) 1210–1221.

[10] C. Kong, J. Ki, M. Kang, A new scaling method for component maps of gas turbine using system identification, J. Eng. Gas Turbines Power 125 (4) (2003) 979–985.

[11] Y. G. Li, P. Pilidis, Ga-based design-point performance adaptation and its comparison with icm-based approach, J. Appl. Energy 87 (1) (2010) 340–348.

[12] R. Ganguli, Gas Turbine Diagnostics: Signal Processing and Fault Isolation, CRC Press, 2012.

[13] E. Tsoutsanis, Y. G. Li, P. Pilidis, M. Newby, Part-load performance of gas turbines: part 1 a novel compressor map generation approach suitable for adaptive simulation, in: Proc. ASME Gas Turbine India, Vol. 1, Mumbai, India, 2012, pp. 733–742.

[14] PROOSIS, Propulsion Object-Oriented Simulation Software, see also `http://www.proosis.com/` (2014).

[15] E. Tsoutsanis, N. Meskin, M. Benammar, K. Khorasani, Dynamic performance simulation of an aeroderivative gas turbine using the matlab simulink environment, in: Proc. ASME IMECE, Vol. 4, San Diego, USA, 2013, p. V04AT04A050.

[16] E. Tsoutsanis, Y. G. Li, P. Pilidis, M. Newby, Part-load performance of gas turbines: part 2 multi-point adaptation with compressor map generation and ga optimization, in: Proc. ASME Gas Turbine India, Vol. 1, Mumbai, India, 2012, pp. 743–751.

[17] N. Aretakis, G. Doumouras, I. Roumeliotis, K. Mathioudakis, Compressor washing economic analysis and optimization for power generation, J. Appl. Energy 95 (2012) 77–86.

[18] J. Klapproth, M. Miller, D. Parker, Aerodynamic development and performance of the cf6-6/lm2500 compressor, in: Proc. 4th International Symposium on Air Breathing Engines, Orlando, USA, 1979, pp. 243–249.

[19] P. K. Zachos, I. Aslanidou, V. Pachidis, R. Singh, A sub-idle compressor characteristic generation method with enhanced physical background, J. Eng. Gas Turbines Power 133 (8) (2011) 081702.

[20] A. J. Fawke, H. I. H. Saravanamuttoo, Digital computer methods for prediction of gas turbine dynamic response, Tech. rep., SAE Technical Paper (1971).

[21] MATLAB, version 8.3 (R2014a), The MathWorks Inc., Natick, Massachusetts, 2014.

[22] J. Lagarias, J. Reeds, M. Wright, P. Wright, Convergence properties of the nelder–mead simplex method in low dimensions, SIAM Journal on optimization 9 (1) (1998) 112–147.

[23] Y. G. Li, P. Nilkitsaranont, Gas turbine performance prognostic for condition-based maintenance, J. Appl. Energy 86 (10) (2009) 2152–2161.